ISSN 1070-3284, Russian Journal of Coordination Chemistry, 2020, Vol. 46, No. 5, pp. 302–307. © Pleiades Publishing, Ltd., 2020.
Russian Text © The Author(s), 2020, published in Koordinatsionnaya Khimiya, 2020, Vol. 46, No. 5, pp. 264–269.

Supramolecular Bromoantimonate(V) Polybromide $(2,6\text{-BrPyH})_3[SbBr_6]\{(Br_2)Br\} \cdot 2H_2O$: Specific Features of Halogen···Halogen Contacts in the Crystal Structure

M. A. Bondarenko[a], S. A. Adonin[a, b, c, d, *], A. S. Novikov[e], M. N. Sokolov[a, d], and V. P. Fedin[a, d]

[a] *Nikolaev Institute of Inorganic Chemistry, Siberian Branch, Russian Academy of Sciences, Novosibirsk, 630090 Russia*
[b] *Tyumen Industrial University, Tobolsk Industrial Institute (Branch), Tobolsk, Russia*
[c] *Southern Ural State University, Chelyabinsk, Russia*
[d] *Novosibirsk National Research University, Novosibirsk, 630090 Russia*
[e] *St. Petersburg State University, St. Petersburg, 199164 Russia*
**e-mail: adonin@niic.nsc.ru*

Received November 1, 2019; revised November 15, 2019; accepted November 26, 2019

Abstract—The reaction of a solution of Sb_2O_3 in HBr in the presence of Br_2 with a solution of 2,6-dibromopyridine (2,6-BrPy) in HBr affords supramolecular bromoantimonate polybromide $(2,6\text{-BrPy})_3[SbBr_6]\{(Br_2)Br\} \cdot 2H_2O$ (**I**). The structure of compound **I** is determined by X-ray structure analysis (CIF file CCDC no. 1962867). The energies of noncovalent Br···Br interactions in the solid state are estimated by quantum-chemical calculations.

Keywords: antimony, halogen bond, halide complexes, noncovalent interactions, quantum-chemical calculations

DOI: 10.1134/S1070328420040016

INTRODUCTION

Increasing interest in the chemistry of halide complexes of *p* elements (Pb, Sb, Bi, and others) [1–3] is caused, to a significant extent, by the possibility of using them as components of solar cells of the so-called perovskite type [4–10]. We have recently shown that bromoantimonates(V) can also play this role, and the efficiency of the first model devices based on $(1\text{-EtPy})[SbBr_6]$ reaches 4% [11]. The Sb(V) bromide complexes can be synthesized using the general scheme: $[Sb^{III}Br_6]^{3-} + Br_2 + CatBr_x + HBr$ (Cat is an organic cation). However, the diversity of products of these reactions is not restricted by the mononuclear complex $Cat[Sb^{V}Br_6]$ only. The factor predetermining the structures and compositions of the formed compounds is the nature of the cation, the salt of which is used in the synthesis [12, 13]. Diverse variants can take place during the reactions: Sb(III) can undergo the complete or partial oxidation to Sb(V). The polybromide fragments forming, as a rule, halogen bonds [14–16] with bromoantimonate(V) anions in the solid state and leading to one-, two-, or three-dimensional supramolecular associates [17–20] can enter or not into the structure of the complex simultaneously with the oxidation to Sb(V). We have previously shown [12] that the use of bromide salts of the pyridinium derivatives (Py) as reagents in the above indicated scheme can give complexes containing up to eleven Br atoms per Sb atom. It was also mentioned for halogen-containing Py [12, 21] that the noncovalent halogen···halogen contacts involving the cations take place in the crystal packing in some cases. Continuing this series of experiments, we synthesized bromoantimonate polybromide $(2,6\text{-BrPyH})_3[SbBr_6]\{(Br_2)Br\} \cdot 2H_2O$ (**I**) using 2,6-dibromopyridine as a precursor. The structure of complex **I** was determined by X-ray structure analysis. The energies of the noncovalent Br···Br interactions in the structure of compound **I** were estimated using quantum-chemical calculations.

EXPERIMENTAL

The synthesis was carried out in air. The initial reagents were purchased from commercial sources. The operation with solutions of Br_2 requires the necessary fulfillment of caution measures. Concentrated HBr (reagent grade) was used.

Synthesis of $(2,6\text{-BrPyH})_3[SbBr_6]\{(Br_2)Br\} \cdot 2H_2O$ (I). Antimony oxide Sb_2O_3 (37 mg, 0.13 mmol) was dissolved in HBr (3 mL), and the following reagents were consequently added: a 1 M solution (1.5 mL) of Br_2 in HBr and a solution of 2,6-dibromopyridine (60 mg, 0.25 mmol) in HBr (1 mL). The

Table 1. Crystallographic data and structure refinement parameters for compound **I**

Parameter	Value
Empirical formula	$C_{15}H_{16}N_3O_2Br_{21}Sb_2$
FW	2191.92
Crystal system	Monoclinic
Space group	*C*2/*c*
a, Å	32.8242(9)
b, Å	9.6155(2)
c, Å	14.7877(4)
β, deg	101.732(3)
V, Å^3	4569.8(2)
Z	4
ρ_{calc}, g/cm^3	3.186
μ, mm^{-1}	19.57
F(000)	3920
Crystal size, mm	0.41 × 0.34 × 0.32
Scan range over θ, deg	29.0–3.3
Range of indices *hkl*	$-32 \le h \le 44$, $-13 \le k \le 12$, $-19 \le l \le 20$
Number of measured/ independent reflections	16 416/5262
R_{int}	0.039
Number of reflections with $I > 2\sigma(I)$	4480
R ($F^2 > 2\sigma(F^2)$), wR (F^2), S	0.034, 0.080, 1.06
$\Delta\rho_{max}/\rho_{min}$, e Å^{-3}	1.46/–1.73

mixture was kept on cooling (6°C) for 24 h, and cherry-black crystals of compound **I** were formed. The yield was 76%.

For $C_{15}H_{16}N_3O_2Br_{21}Sb_2$			
Anal. calcd., %	C, 8.2	H, 0.7	N, 1.9
Found, %	C, 8.3	H, 0.7	N, 2.0

X-ray structure analysis of complex **I** was conducted at 130 K on an Agilent Xcalibur automated diffractometer equipped with an Atlas S2 two-coordinate detector (graphite monochromator, λ(MoK_α) = 0.71073 Å, ω scan mode). The integration was performed, an absorption correction was applied, and the unit cell parameters were determined using the CrysAlisPro program package. The crystal structures were solved using the SHELXT program and refined by full-matrix least squares in the anisotropic (except for hydrogen atoms) approximation using the SHELXL program [22]. The positions of the hydrogen atoms of the organic ligands were calculated geometrically and refined by the riding model. The crystallographic data and details of X-ray diffraction experiments are presented in Table 1.

The full tables of interatomic distances and bond angles, coordinates of atoms, and atomic shift parameters were deposited with the Cambridge Crystallographic Data Centre (CIF file CCDC no. 1962867; https://www.ccdc.cam.ac.uk/structures/).

Quantum-chemical calculations were performed in the framework of the density functional theory (M06/DZP-DKH) [23–25] using the Gaussian-09 program package.

RESULTS AND DISCUSSION

As mentioned above, the compositions and structures of the complexes synthesized via the general scheme $[Sb^{III}Br_6]^{3-} + Br_2 + CatBr_x + HBr$ are predetermined by the nature of $CatBr_x$. The first works devoted to the structural characterization of these reaction products were published in the late 1960s–early 1970s [18–20, 26, 27], and later we additionally described more than 20 compounds [12, 21, 28].

The coordination environment of Sb in the $[Sb^VBr_6]^-$ anions in compound **I** represents a slightly distorted octahedron, and the Sb–Br bond lengths are typical of bromoantimonates(V) (2.527–2.563 Å). The structure contains the dibromine fragments (Br–Br 2.377 Å) bound to each other by the bromide anions (Br(35)···Br(34) 2.956 Å; hereinafter, for the designation of Br atoms, see Table 2) into infinite polymer chains $\{(Br_2)Br\}_n^{n-}$, and similar structural motifs were described previously for polybromide salts of a number of organic cations [29]. The unusual feature of compound **I** is the presence of solvate H_2O molecules (two molecules per formula unit).

The system of noncovalent Br···Br interactions in the structure of compound **I** is very complicated, because the bromine atoms belonging to both the $[Sb^VBr_6]^-$ and $\{(Br_2)Br\}_n^{n-}$ anions and 2,6-dibromopyridinium cations are involved in structure formation. Each of the bromoantimonate(V) anions interacts with three adjacent cations (Br···Br 3.453–3.582, Br(5)···Br(32), and Br(4)···Br(14) Å are contacts of type 1) and one 2,6-$BrPyH^+$ cation (Br···Br 3.504 Å (Br(18)···Br(5), type 2)). In turn, the 2,6-$BrPyH^+$ cation forms contacts with the bromide anion in the composition of the $\{(Br_2)Br\}_n^{n-}$ chains (Br···Br 3.369 Å (Br(15)···Br(34), type 2)). On the whole, all Br···Br interactions lead to the formation of the three-dimensional structure (Figs. 1–3).

Table 2. Electron density ($\rho(\mathbf{r})$), Laplacian electron density ($\nabla^2\rho(\mathbf{r})$), total energy density (H_b), potential energy density ($V(\mathbf{r})$), and Lagrangian kinetic energy ($G(\mathbf{r})$) (atomic units) at the critical bond points (3, –1) corresponding to the noncovalent Br···Br interactions in the crystal of compound **I** and the lengths of these contacts (l, Å) and their energies (E, kcal/mol) estimated using various correlations proposed in the literature

Supramolecular contact[a]	$\rho(\mathbf{r})$	$\nabla^2\rho(\mathbf{r})$	H_b	$V(\mathbf{r})$	$G(\mathbf{r})$	E^b	E^c	E^d	E^e	l^f
Br(5)···Br(32) (type 1)	0.011	0.027	0.000	–0.006	0.006	1.9	1.6	2.2	2.1	3.453
Br(4)···Br(14) (type 1)	0.010	0.023	0.000	–0.005	0.006	1.6	1.6	1.8	2.1	3.582
Br(35)···Br(34) (type 2)	0.028	0.061	0.000	–0.015	0.015	4.7	4.0	5.5	5.4	2.956
Br(15)···Br(34) (type 2)	0.007	0.019	0.000	–0.004	0.004	1.3	1.1	1.5	1.4	3.369
Br(18)···Br(5) (type 2)	0.009	0.026	0.001	–0.005	0.006	1.6	1.6	1.8	2.1	3.504

[a] The classification according to types of the supramolecular contacts involving halogen atoms was discussed in detail [14].
[b] $E = -V(\mathbf{r})/2$ (correlation was developed for the estimation of the energy of hydrogen bonds) [41].
[c] $E = 0.429G(\mathbf{r})$ (correlation was developed for the estimation of the energy of hydrogen bonds) [42].
[d] $E = 0.58(-V(\mathbf{r}))$ (correlation was specially developed for the estimation of the energy of noncovalent interactions involving bromine atoms) [43].
[e] $E = 0.57G(\mathbf{r})$ (correlation was specially developed for the estimation of the energy of noncovalent interactions involving bromine atoms) [43].
[f] The shortest van der Waals radius for the bromine atom is 1.83 Å [44].

In order to estimate the energies of the aforementioned contacts, we performed the quantum-chemical calculations (for details, see above) and topological analysis of the electron density distribution using the QTAIM method [30] (this approach is widely used for studying the properties of noncovalent interactions of various types [31–38]). The results are presented in Table 2, and the diagrams of contour lines of the Laplacian electron density distribution $\nabla^2\rho(\mathbf{r})$, bonding routes, and zero flux surfaces corresponding to various noncovalent Br···Br interactions in the crystal of compound **I** are presented in Fig. 4. The values of the electron density, Laplacian electron density, total energy density, potential energy density, and Lagrangian kinetic energy at the critical bond points (3, –1) corresponding to the noncovalent Br···Br interactions in the crystal of compound **I** are quite typical of supramolecular contacts of this type involving halogen atoms [39, 40]. The estimation values of the energy of the noncovalent Br···Br interactions in the crystal of compound **I** vary in a range of 1.1–5.5 kcal/mol depending in the type of the contact and can differ (by up to 0.5 kcal/mol, see Table 2) for different estimation methods. However, the energies of the Br···Br contacts between various fragments are comparable, which is consistent with our earlier observations [28].

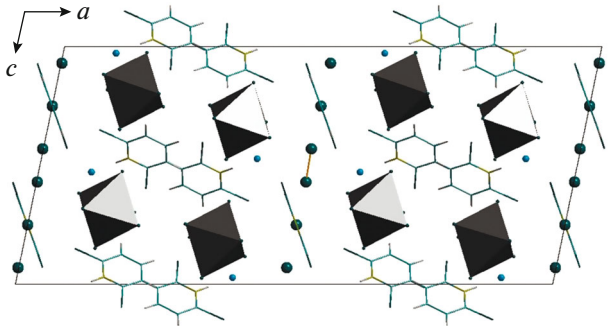

Fig. 1. Packing of the cations and anions in the structure of compound **I**. The cations are shown in the "wire-and-stick" model, and the $[SbBr_6]^-$ anions are presented as polyhedra.

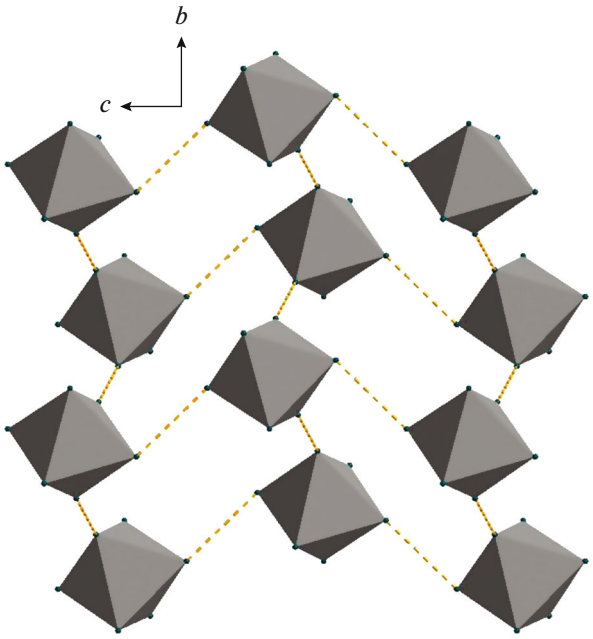

Fig. 2. Contacts Br···Br (shown by dashed lines) between the bromide ligands of the $[SbBr_6]^-$ anions (shown as polyhedra) in the structure of compound **I**.

The ratio of the potential energy density and Lagrangian kinetic energy at the critical bond points (3, −1) corresponding to the noncovalent Br···Br interactions in the crystal of compound **I** indicates the absence of a substantial fraction of the covalent component in these supramolecular contacts.

FUNDING

The experimental part of the work (synthesis and structural characterization) was supported by the Russian Science Foundation, project no. 18-73-10040. The theoretical studies (quantum-chemical calculations and topological analysis of the electron density distribution using the

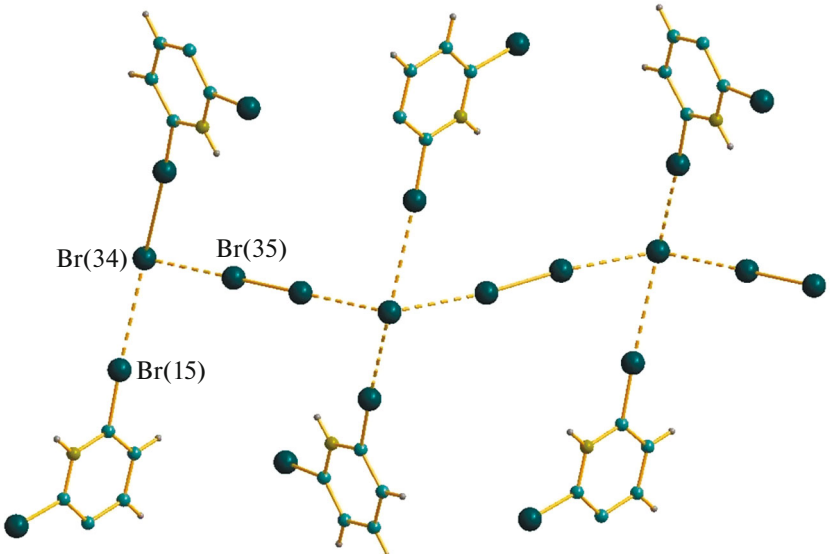

Fig. 3. Contacts Br···Br (shown by dashed lines) between the polybromide $\{(Br_2)Br\}_n^{n-}$ fragments and 2,6-$BrPyH^+$ cations in the structure of compound **I**.

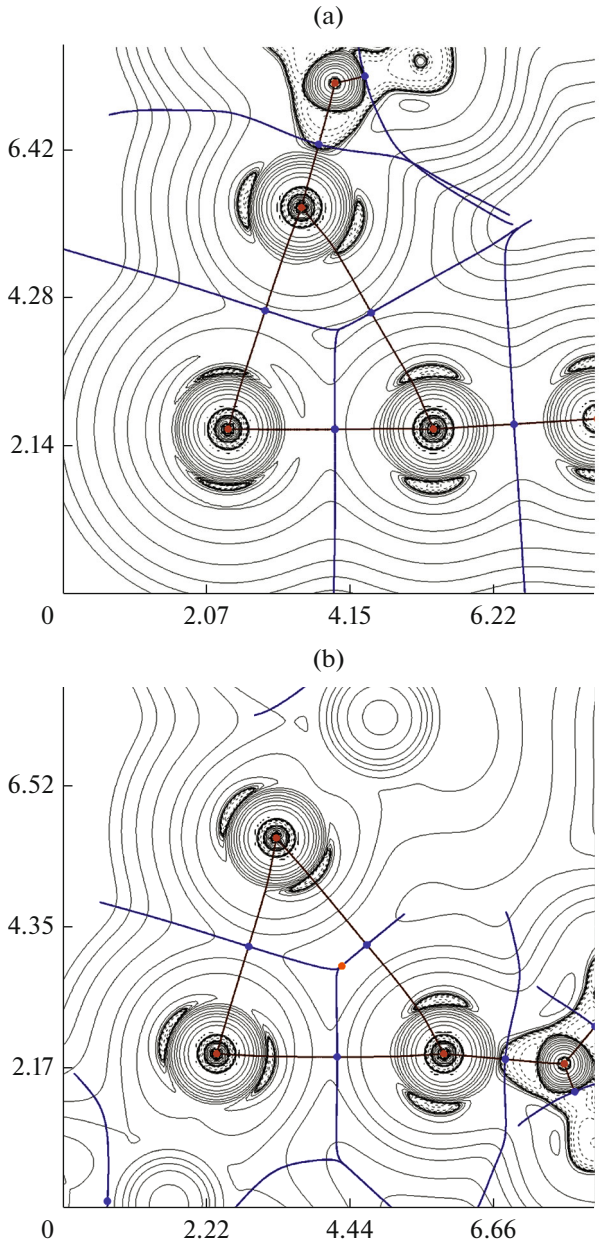

Fig. 4. Diagram of contour lines of the Laplacian electron density distribution $\nabla^2\rho(\mathbf{r})$, bonding routes, and zero flux surfaces corresponding to the noncovalent interactions (a) Br(35)···Br(34) and Br(15)···Br(34) and (b) Br(5)··· Br(32) and Br(18)···Br(5) in the crystal of compound **I**. The critical bond points (3, −1) are blue, critical nuclei points (3, −3) are light brown, and critical points of the cycle (3, +1) are orange. The length units are Å.

QTAIM method) were supported by the Russian Science Foundation, project no. 19-73-00001.

CONFLICT OF INTEREST

The authors declare that they have no conflicts of interest.

REFERENCES

1. Buikin, P.A., Rudenko, A.Y., Baranchikov, A.E., et al., *Russ. J. Coord. Chem.,* 2018, vol. 44, p. 373. https://doi.org/10.1134/S1070328418060015
2. Kotov, V.Y., Ilyukhin, A.B., Simonenko, N.P., et al., *Polyhedron*, 2017, vol. 137, p. 122.
3. Sharutin, V.V., Sharutina, O.K., Khisamov, R.M., et al., R*uss. J. Inorg. Chem.*, 2017, vol. 62, p. 766. https://doi.org/10.1134/S0036023617060201
4. Frolova, L.A., Dremova, N.N., and Troshin, P.A., *Chem. Commun.*, 2015, vol. 51, p. 14917.
5. Park, B.-W., Philippe, B., Zhang, X., et al., *Adv. Mater.*, 2015, vol. 27, p. 6806.
6. Ganose, A.M., Savory, C.N., and Scanlon, D.O., *Chem. Commun.*, 2017, vol. 53, p. 20.
7. Frolova, L.A., Anokhin, D.V., Piryazev, A.A., et al., *J. Phys. Chem. Lett.*, 2017, vol. 8, p. 1651.
8. Frolova, L.A., Anokhin, D.V., Piryazev, A.A., et al., *J. Phys. Chem. Lett.*, 2017, vol. 8, p. 672.
9. Shestimerova, T.A., Golubev, N.A., Yelavik, N.A., et al., *Cryst. Growth Des.*, 2018, vol. 18, p. 2572.
10. Shestimerova, T.A., Yelavik, N.A., Mironov, A.V., et al., *Inorg. Chem.*, 2018, vol. 57, p. 4077.
11. Adonin, S.A., Frolova, L.A., Sokolov, M.N., et al., *Adv. Energy Mater.*, 2018, vol. 8, p. 1701140.
12. Adonin, S.A., Bondarenko, M.A., Novikov, A.S., et al., *CrystEngComm*, 2019, vol. 21, p. 850.
13. Adonin, S.A., Bondarenko, M.A., Abramov, P.A., et al., *Russ. J. Coord. Chem.,* 2019, vol. 45, p. 128. https://doi.org/10.1134/S1070328419020027
14. Cavallo, G., Metrangolo, P., Milani, R., et al., *Chem. Rev.*, 2016, vol. 116, p. 2478.
15. Torubaev, Y.V., Rai, D., Skabitsky, I.V., et al., *New J. Chem.*, 2019, vol. 43, p. 7941.
16. Torubaev, Y.V., Skabitskiy, I.V., Rusina, P., et al., *CrystEngComm*, 2018, vol. 20, p. 2258.
17. Hubbard, C.R. and Jacobson, R.A., *Inorg. Chem.*, 1972, vol. 11, p. 2247.
18. Lawton, S.L., McAfee, E.R., Benson, J.E., et al., *Inorg. Chem.*, 1973, vol. 12, p. 2939.
19. Lawton, S.L. and Jacobson, R.A., *Inorg. Chem.*, 1968, vol. 7, p. 2124.
20. Lawton, S.L. and Jacobson, R.A., *Inorg. Chem.*, 1971, vol. 10, p. 709.
21. Adonin, S.A., Bondarenko, M.A., Samsonenko, D.G., et al., *J. Mol. Struct.*, 2018, vol. 1160, p. 102.
22. Sheldrick, G.M., *Acta Crystallogr., Sect. C: Struct. Chem.*, 2015, vol. 71, p. 3.
23. Zhao, Y. and Truhlar, D.G., *Theor. Chem. Acc.*, 2008, vol. 120, p. 215.
24. Barros, C.L., de Oliveira, P.J.P., Jorge, F.E., et al., *Mol. Phys.*, 2010, vol. 108, p. 1965.
25. Canal Neto, A. and Jorge, F.E., *Chem. Phys. Lett.*, 2013, vol. 582, p. 158.
26. Lawton, S.L., Hoh, D.M., Johnson, R.C., et al., *Inorg. Chem.*, 1973, vol. 12, p. 277.
27. Lawton, S.L., Jacobson, R.A., and Frye, R.S., *Inorg. Chem.*, 1971, vol. 10, p. 701.

28. Adonin, S.A., Bondarenko, M.A., Abramov, P.A., et al., *Chem.-Eur. J.*, 2018, vol. 24, p. 10165.
29. Haller, H. and Riedel, S., *Z. Anorg. Allg. Chem.*, 2014, vol. 640, p. 1281.
30. Bader, R.F.W., *Chem. Rev.*, 1991, vol. 1, p. 893.
31. Andrusenko, E.V., Novikov, A.S., Starova, G.L., et al., *Inorg. Chim. Acta*, 2016, vol. 447, p. 142.
32. Novikov, A.S., Ivanov, D.M., Bikbaeva, Z.M., et al., *Cryst. Growth Des.*, 2018, vol. 18, p. 7641.
33. Kinzhalov, M.A., Kashina, M.V., Mikherdov, A.S., et al., *Angew. Chem., Int. Ed. Engl.*, 2018, vol. 7, p. 12785.
34. Bulatova, M., Melekhova, A.A., Novikov, A.S., et al., *Z. Kristallogr. Cryst. Mater.*, 2018, vol. 33, p. 371.
35. Il'in, M.V., Bolotin, D.S., Novikov, A.S., et al., *Inorg. Chim. Acta*, 2019, vol. 490, p. 267.
36. Burianova, V.K., Bolotin, D.S., Mikherdov, A.S., et al., *New J. Chem.*, 2018, vol. 42, p. 8693.
37. Ding, X., Tuikka, M.J., Hirva, P., et al., *CrystEngComm*, 2016, vol. 18, p. 1987.
38. Mikherdov, A.S., Kinzhalov, M.A., Novikov, A.S., et al., *J. Am. Chem. Soc.*, 2016, vol. 138, p. 14129.
39. Adonin, S.A., Gorokh, I.D., Novikov, A.S., et al., *CrystEngComm*, 2018, vol. 20, p. 7766.
40. Usoltsev, A.N., Adonin, S.A., Novikov, A.S., et al., *CrystEngComm*, 2017, vol. 19, p. 5934.
41. Espinosa, E., Molins, E., and Lecomte, C., *Chem. Phys. Lett.*, 1998, vol. 285, p. 170.
42. Vener, M.V., Egorova, A.N., Churakov, A.V., et al., *J. Comput. Chem.*, 2012, vol. 33, p. 2303.
43. Bartashevich, E.V. and Tsirelson, V.G., *Russ. Chem. Rev.*, 2014, vol. 83, p. 1181.
44. Bondi, A., *J. Phys. Chem.*, 1966, vol. 70, p. 3006.

Translated by E. Yablonskaya